Asian Journal of Green Chemistry

AJGC
Asian Journal of
Green Chemistry

Original Research Article

Synthesis nanoparticles derivations of graphene oxide and poly (Styrene–alternative-maleic anhydride) for removing zinc(II) ions from aqueous solutions

Naser Samadi[a], Reza Ansari[b], Bakhtiar Khodavirdilo[b,*]

[a] *Department of Analytical Chemistry, Faculty of Chemistry, Urmia University, Urmia, Iran*

[b] *Department of Chemistry, Faculty of Science, University of Guilan, University Campus 2, Rasht, Iran*

ARTICLE INFORMATION
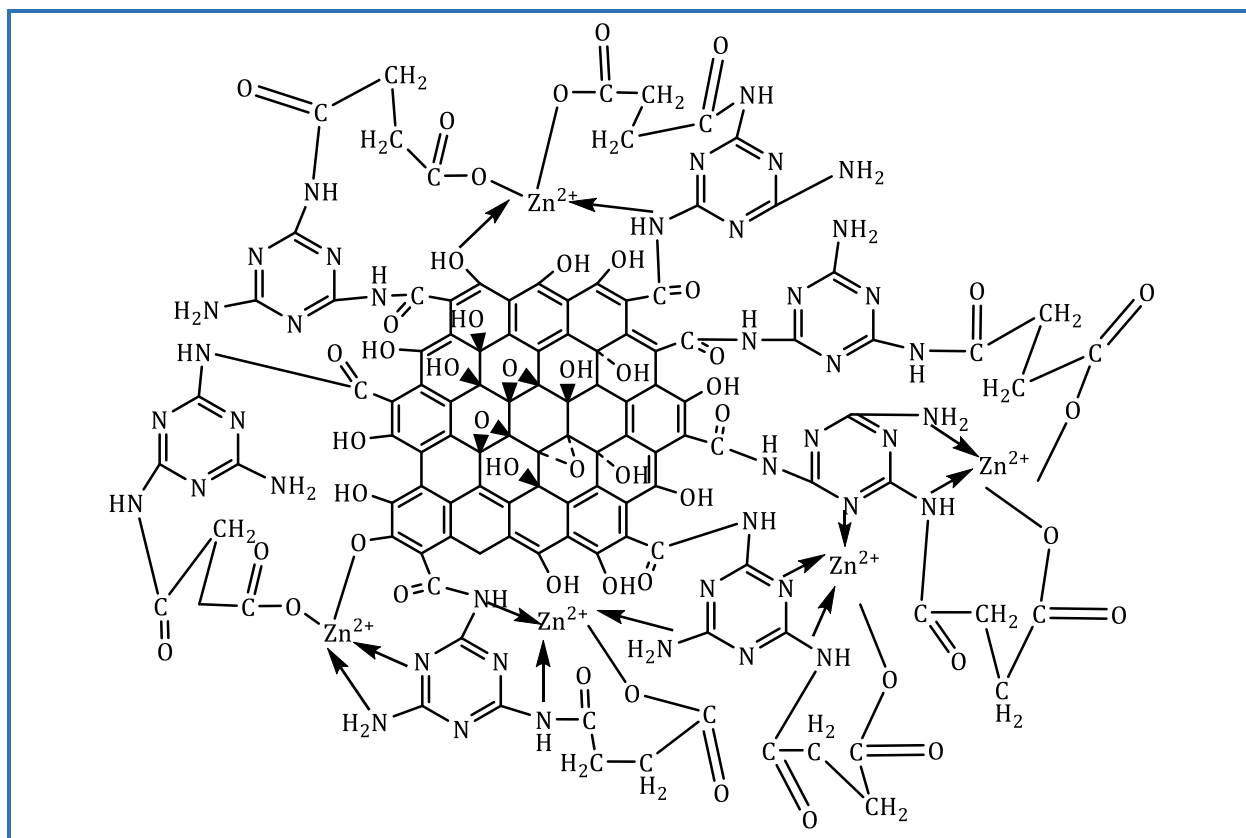
ABSTRACT

In this research, a new method that uses graphene oxide (GO) nanosheets melamine butanedioic acid (GO-MB) composites and derivation of poly (Styrene–alternative-maleic anhydride) (SMA), (SMA + melamine-butanedioic acid) (SMA-MB), as sorbents for the elimination of zinc(II) ions from aqueous solutions, is presented. The adsorbents have the sufficiency to adsorb the zinc(II) ions. Through immobilizing the melamine-butanedioic acid onto GO nanosheets and SMA-MB, the desired composite was synthesized and identified by field emission scanning electron microscopy (FE-SEM) and fourier transform infrared (FT-IR) spectroscopy techniques. Some experimental parameters including, pH, concentration of the aqueous solution of zinc(II) ions, the content of the zinc(II) ions, the grapheme oxide-melamine-butanedioic acid, and SMA-MB were optimized. The results showed that the adsorbents were matched with langmuir isotherm. It was also revealed that the uptake efficiency of zinc(II) ions were considerably increased after immobilization of melamine-butanedioic acid on the GO nanosheets and SMA. These adsorbents were also shown to be very suitable to remove the zinc(II) ions from aqueous solutions.

Corresponding author, email: b_khodavirdilo@yahoo.com (B. Khodavirdilo).
Mobile: +98914 5608319.

Graphical Abstract

Introduction

Environmental impurity has been one of the major objects of any society over the recent decades. The main pollutants contain toxic heavy metals, the quantity of which continually increases in the environment as the consequence of increased industrial activity [1].

Zinc is one of these toxic metals and is present in high concentration in wastewater produced in some industries including, galvanizing, metallurgical, electroplating, mining, painting, pigments, pharmaceuticals, fiber production, ground wood pulp, newsprint paper, batteries, petroleum, and petrochemical [2]. Zinc ions will not be reduced and will be carried away to the food chain and finally get accumulated in the living organisms, causing several diseases and disorders [3–5]. Wastewater remedies would not only be economical but will also help to protect the quality of the environment. The heavy metals, having hazardous impacts on health, can be remedied from wastewater using different physicochemical manners. The diffusion of large quantities of heavy metals into the natural environment has consequences in a number of environmental objects. In recent years, various adsorption processes, such as adsorption, corrected media adsorption, and industrial wastes adsorption, have appeared to be potential alternative manners. Due to low cost and easy-to-get

nature, the industrial wastes as absorbents have been used for the removal of toxic pollutants from wastewater, especially for dyes. Meanwhile, some naturally available adsorbents like hen feathers, and wheat husk were also used for the removal of hazardous dye. However, the above absorbents were seldom used to absorb the heavy metal ions [6–8].

In this study, we used the modified graphene oxide and modified the polystyrene alternative maleic anhydride with oxalic acid in order to remove zinc(II) ion from aqueous solutions. It was prepared and its adsorption conditions were studied by varying the initial pH, temperature, adsorbent dosage, and contact time for zinc(II) ion removal from the administrated wastewater. Therefore, the mechanism of the adsorption was also graced by a series of tests.

Experimental

Materials and methods

All the reagents including, melamine, styrene, maleic anhydride, H_2SO_4, $NaNO_3$, H_2O_2, and $KMnO_4$ were prepared using analytical reagent grade chemicals supplied from Merck (Darmstadt, Germany), except $Zn(NO_3)_2.6H_2O$ which was purchased from aldrich. The 10^{-3} M zinc(II) salt standard stock solution was prepared by dissolving 0.022 g of $Zn(NO_3)_2.6H_2O$ in a 250 mL volumetric flask and diluting to the mark with distilled water. Lower concentrations were prepared by serial dilution of the stock solution with phosphate buffer; pH 8 universal buffer solutions (0.1 M) were prepared from phosphoric acid solutions and sodium hydroxide solutions and adjusting pH to the desired value (0.1 M). The final pH was adjusted with the addition of a sodium hydroxide. The IR spectra were analyzed with a fourier transform infrared spectrophotometer (Nexus-670, Thermo Nicolet, USA). Atomic absorption spectrophotometry (AAS; Analytik jena novAA 400, Germany) was used to determine the heavy metal-ion concentrations in aqueous solutions. The inherent viscosity of the resulting SMA polymer was obtained with an ostwald viscometer at 25 °C in a thermostatic water bath. The elemental analysis of one of the adsorbent was performed by a CHN analyzer (2400 series II, PerkinElmer Co., USA). The morphology of the particles was examined *via* scanning electron microscopy (SEM; XL 30 Philips, Netherland).

Synthesis of melamine–butanedioic acid

To synthesize the grafted SMA polymer, 0.2 gr of melamine was dissolved in pH=4.34 of 15 mL cold water that with adding 0.1 M of HCl adjusted pH in pH=4.34. In the other flask, 1 gr of extra butanedioic acid was dissolved in 15 mL of THF. Then, the dissolved melamine was added slowly to the flask containing butanedioic acid, that was clear at first and then it was formed turbid, and produced mixture along with vigorous magnetic stirring. The obtained product was filtered and
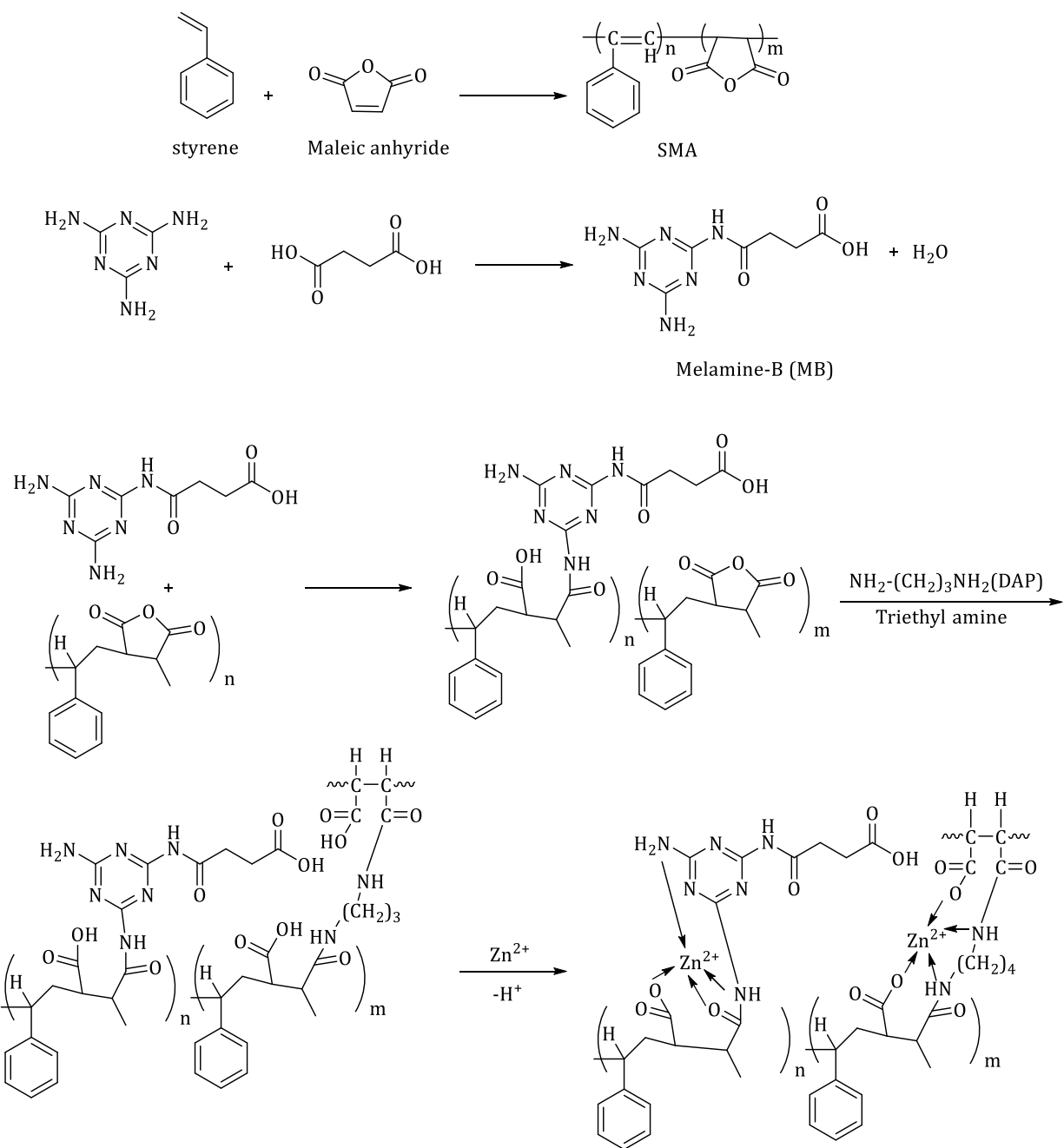
heated up to vaporize the THF. The beaker was put in a refrigerator to form the crystal (Melamine-butanedioic acid) (MB). The SMA polymer was prepared by the free-radical polymerization of maleic anhydride and styrene at 72 °C at the presence of the benzoyl peroxide as an initiator. To synthesize the grafted SMA polymer, 1.5 g (0.0075 mol) of SMA polymer and 0.8875 g (0.00375 mol) of melamine-butanedioic acid (MB) at a ratio of 1:0.5 were poured into a flask. Then, 0.5 mL (0.004 mol) of tri ethylamine (TEA) as a catalyst and 50 mL of THF as a solvent were charged in a three necked, round-bottom flask equipped with a condenser, magnetic stirring bar, inlet and outlet for inert gas, and ultrasonic irradiation probe. The reaction mixture was refluxed under these conditions for 6 h at 95 °C. The precipitations were completed by adding the *n*-hexane as a nonsolvent, and then separated using a filter and washed by *n*-hexane several times. The product was dried in a vacuum oven for 10 h at 64 °C (Yield=99%). The synthesis process of the chelating resin is shown in (Scheme 1). The FT-IR spectra of the CSMA-MB is shown in (Figure 1) [9−12].

Synthesis of graphene oxide nanosheets (GO)

Graphene oxide was prepared using a modified Hummers and Foeman's method. Briefly in a typical reaction, 1 g graphite, 1 g $NaNO_3$, and 46 mL H_2SO_4 were stirred together in an ice bath. $KMnO_4$ (8 g) was slowly added while stirring, and the rate of addition was controlled to prevent the mixture temperature from exceeding 20 °C. The mixture was then transferred to a 35 °C water bath and stirred for about 1 h, forming a thick paste. Subsequently, 80 mL of deionized water was gradually added and the temperature was raised to 90 °C. The mixture was further treated with 10 mL 30% H_2O_2 solution. The solution was then filtered and washed with deionized water until the pH was 6 and, finally, dried at 65 °C under vacuum (Scheme 2) [13−15].

Synthesis of covalently attached MB graphene oxide hybrids (GO-MB)

Briefly, in a typical reaction, a mixture of 30 mg GO and 60 mg MB was taken in a 100 mL round bottom flask and 4 mL of triethylamine and 20 mL of DMF were added and heated to 82 °C for 62 h under a nitrogen atmosphere. After the reaction, the solution was cooled to room temperature, and then poured into 250 mL diethyl ether to precipitate the product. The precipitate was collected by centrifuging at 8100 rpm for 25 min. The supernatant which contained the dissolved MB was discarded and the precipitate was washed thoroughly. After adding another 100 mL of diethyl ether, the mixture was sonicated for 5 min and then centrifuged at 8100 rpm for 25 min to collect the GO-MB. Finally, the precipitate was washed with $CHCl_3$ four times following the above procedure (Scheme 3) [16−18].
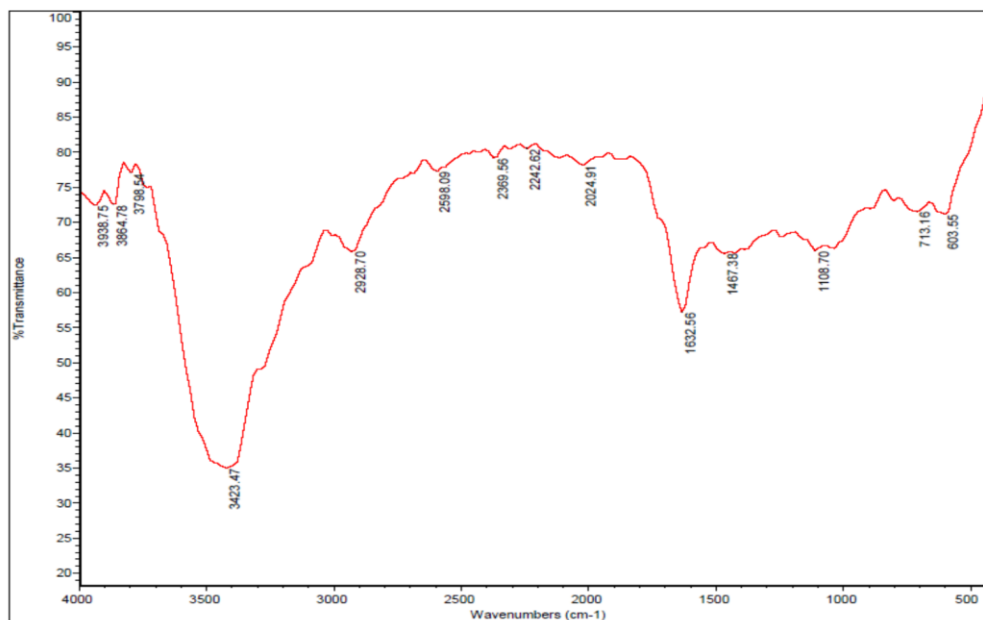
Scheme 1. Synthesized polymers for adsorption of zinc (II) ions
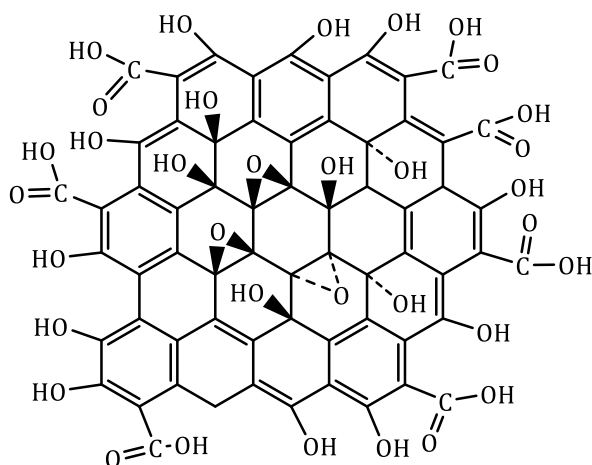
Results and discussion

Structural and spectroscopic characterization of GO-MB and CSMA-MB

The FT-IR spectra were recorded using KBr plates in the range 500-4000 cm^{-1} using a nicolet 6700 FT-IR spectrometer. Figure 1 shows the typical FT-IR spectrum obtained for GO, Go-MB and SMA-

MB. The most significant characteristic features are the broad, intense band at 3435 cm^{-1} (O−H stretching vibrations).

Figure 1. FT-IR spectral of CSMA-MB

Scheme 2. Structural formula of graphene oxide (GO)

and the bands at 1741 cm^{-1} (C=O stretching vibrations from carbonyl and carbamide groups), 1681 cm^{-1} (Skeletal vibrations from unoxidized graphitic domains), 1388 cm^{-1} (C−OH stretching vibrations), and 1040 cm^{-1} (C−O is stretching vibrations). The appearance of the peaks at around 2920 cm^{-1} is ascribed to the aromatic stretching vibrations of C−H bonds of GO. After covalent functionalization with melamine, a new peak appears at 1588 cm^{-1} corresponding to the C=C

vibrations of melamine and the peak of the C–O stretches vibration which shifts to 1212 cm^{-1}, and broadens. The disappearance of the peak at 2382.78 cm^{-1} (C=O from CO_2 stretching vibrations) clearly indicates that in GO-melamine butanedioic acid composite, the melamine molecules are covalently bonded to the GO *via* amine linkage. The SEM image (Figure 2) shows that few layered GO is formed, although the SEM image does not surmise the layer numbers of the GO nanosheets precisely. Pure graphite presents ordered flakes of a 3-4 μm range. The scanning electron micrograph for the GO-melamine butanedioic acid hybrid materials (Figure 2) clarified that a homogeneous system with a micrometer order of magnitude was gained on functionalization. In this sense, GO presents a three-dimensional network of randomly oriented sheet-like structures with a wrinkled texture and hierarchical pores with a wide size distribution.
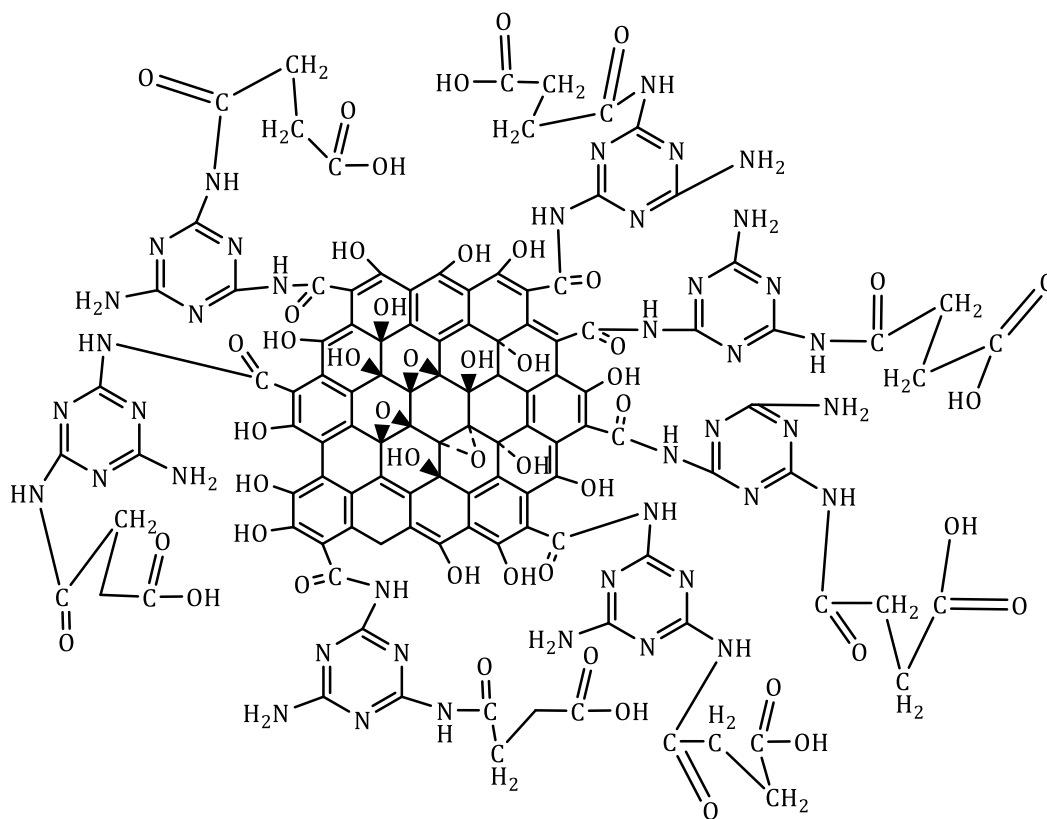
Effect of pH on Zn(II) ion adsorption

pH of the aqueous solutions is one of the most significant controlling parameters that affects the elimination percentage of the Zn(II) ions on adsorbent. The effect of pH on the adsorption of Zn(II) ions was investigated by changing the pH of the Zn(II) ion solution din the range of 1-10 because these Zn(II) ions could be precipitated by OH$^-$ to form Zn(II) hydroxide above pH 8 (K_{sp} for Zn(OH)$_2$ is 5×10^{-17}). The results were depicted in (Figure 3). The extractability of the Zn(II) ions from the solution phase depends on the pH, because it affects the solubility of the Zn(II) ions in water, concentration of the counter ions on the functional groups of adsorbents, and the degree of ionization of the adsorbate during the reaction is very important. The results exhibited that there is approximately no adsorption at pH=0, and the removal percentage of the CSMA-MB and GO-MB for Zn(II) ions increased significantly with increasing the pH. The maximum removal efficiencies of the Zn(II) ions by CSMA-MB and GO-MB were 98.92%, and 98.95%, respectively. An acidic pH, the adsorbent surface will be completely covered with hydronium ions which strongly with Zn(II) ions for adsorption sites at acidic pH, with an increase in pH, the concentration of H_3O^+ ions decreases facilitating the absorption of Zn(II) ions by the adsorbents. The optimized pH for removing zinc(II) ions by CSMA-MB and GO-MB is pH=6 and pH=8, respectively.
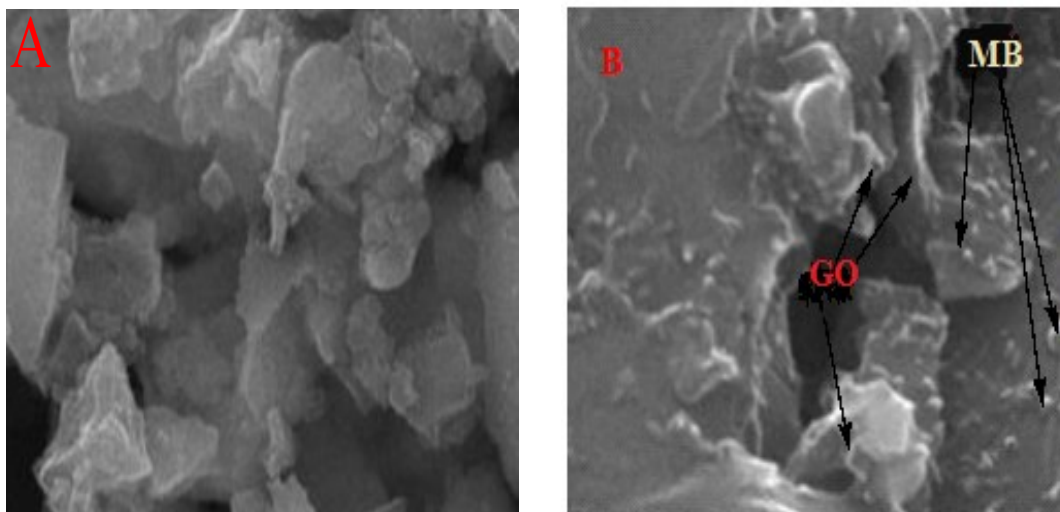
Effect of contact time on zinc(II) ion adsorption

Contact time plays a significant role in the adsorption of Zn(II) ion with solid surface. Elimination percentage of Zn(II) ion is found to be suitable to contact the time up to the achieved equilibrium, after which it is free of time due to the verity that at equilibrium the rate of adsorption and desorption will be same. The effect of contact time for the removal of Zn(II) ion by the CSMA-MB resin and GO-MB showed rapid adsorption of these Zn(II) ions in the first 10 min and, thereafter, the absorption
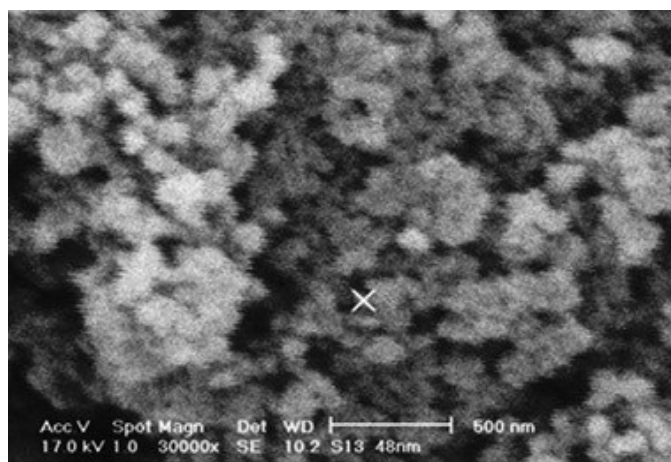
rate reduced gradually and the adsorption arrived equilibrium in about 10–80 min as shown in (Figure 4). The relatively fast sorption of Zn(II) ion on the CSMA-MB resin and GO-MB probably reflects a high availability of the Zn(II) ion to the ion exchange sites in the CSMA-MB and GO-MB. Optimized contact time for removing zinc(II) ions by CSMA-MB and GO-MB is 60 min and 30 min, respectively.
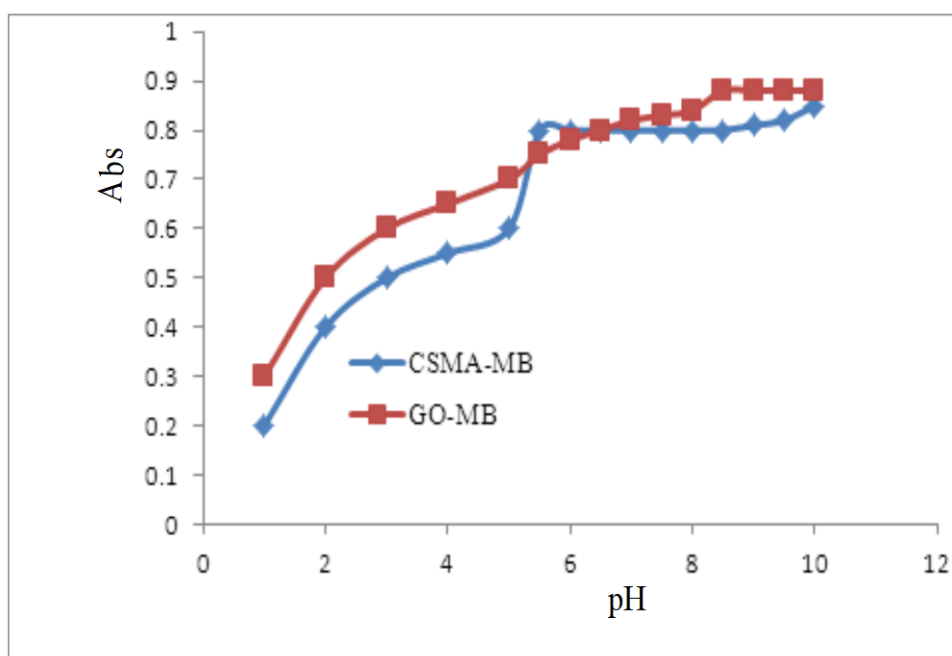

Scheme 3. Structural formula of graphene oxide-melamine butandioic acid (GO-MB)

Figure 2. SEM images of a) graphene oxide nano sheets and b) graphene oxide-melamine butanedioic acid composite and c) CSMA-MB
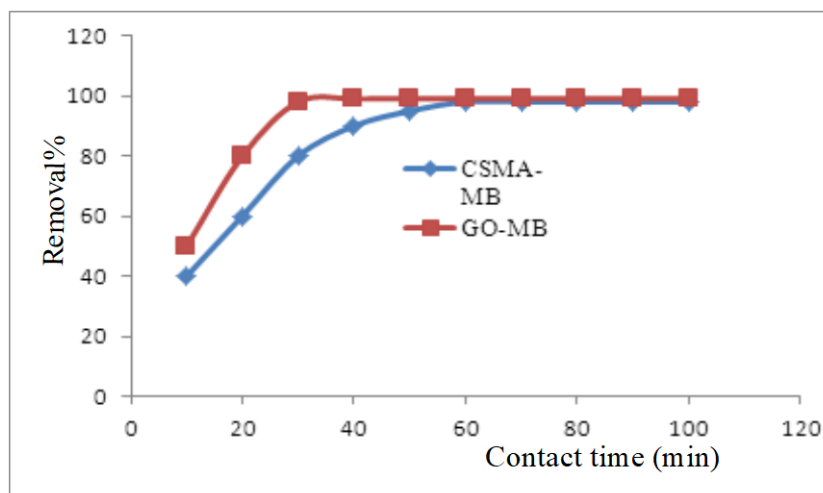

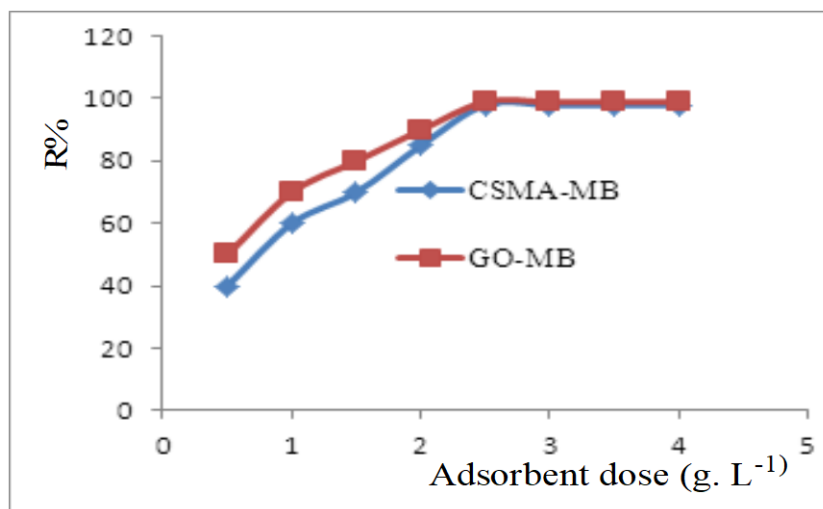**Figure 3.** Effect of pH on zinc(II) ion adsorbents by CSMA-MB and GO-MB

Effect of adsorbents dose on Zn(II) ions adsorptions

The effect of adsorbent dosage is an important factor on the removal percentage of Zn(II) ions from aqueous solutions, because it measures the capacity of an adsorbent for a given concentration. The adsorption efficiency of the Zn(II) ions as a function of adsorbent dosage was surveyed and the effects can be exhibited in (Figure 5). The tentative data showed that the elimination efficiency of the Zn(II) ions increased gradually with increasing the amounts of CSMA-MB and GO-MB. This may be attributed to the reality that increasing the adsorbent dose ready more adsorption sites for the Zn(II)

ions. By increasing the adsorbent dose for Zn(II) ions from 0.5 to 4.0 g/L, the absorption of zinc(II) ion was increased from 85.25% to 99.98% by GO-MB and 85.72% to 95.48%, by CSMA-MB. Effect of concentration of Zn(II) ions on the adsorption. The rate of adsorption is a function of the concentration of Zn(II) ions, which makes it a significant parameter to be supposed for efficient adsorption [19].

Figure 4. Effect of contact time on Zinc(II) ion adsorbents by CSMA-MB and GO-MB

Figure 5. Effect of adsorbent dosage on Zinc(II) ion adsorbents by CSMA-MB and GO-MB

Effect of concentration of zinc(II) ion

The rate of adsorption is a function of the concentration of Zn(II) ion, which makes it a significant parameter to be supposed for efficient adsorption. The effect of Zn(II) ion concentration was surveyed on the adsorption comport of CSMA-MB resin and GO-MB at various concentrations (10-

300 mg/L), and the effects are shown in Figure 6. Generally, Figure 6 exhibits that, by increasing the Zn(II) ion concentration with constant content of the adsorbent, the Zn(II) ion adsorption was increased up to 100 mg/L for Zn(II) ion. Further increases in the Zn(II) ion concentration were accompanied by a reduction in the elimination percentage. This phenomenon might be due to saturation of the active sites of the CSMA-MB and GO-MB with the Zn(II) ion at higher concentrations. We can conclude that these adsorbents have so many active ion exchange sites for elimination of Zn(II) ion from aqueous solution [20].

Effect of agitation speed on adsorption of zinc(II) ions

The effect of agitation speed was investigated under the specified conditions (At the optimum contact time of 1 h for CSMA-MB and 30 min for GO-MB, 100 mg/L^{-1}, 20 mL solution 50 mg/L, pH=6 for CSMA-MB, pH=8 for GO-MB, and at a room temperature of 26 °C) with CSMA-MB and GO-MB as adsorbents, an increase in agitation speed from 50 to 300 rpm was observed, and the elimination percentage of elimination increased up to 300 rpm as shown in (Figure 7). Hence, at an agitation speed of 200 rpm, maximum recoveries were gained for the zinc(II) ions, with 98.25% removal of Zn(II). Also, zinc(II) ions attained maximum removal of 96.51% at a lower agitation speed of 150 rpm. The increase in agitation speed out, coming to increase in zinc(II) ions elimination percentage, was due to the fact that the increase in stirring rate took up the zinc(II) ions diffusion to the surface of the adsorbents; and also caused a decrease in the film boundary layer around the adsorbents [21].
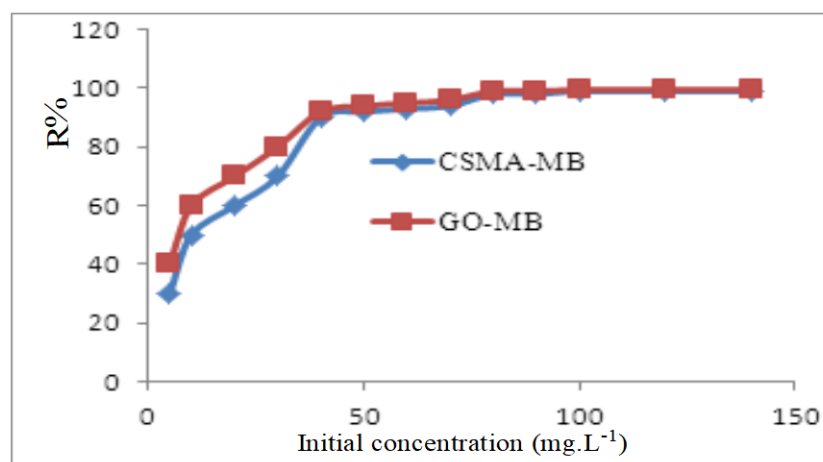
Swelling index

The adsorbent swelled free of any dissolving after being stirred in water. The swelling index of the polymer is exhibited in (Figure 8). The effects clearly represented that the uptake of water depended on the structural characterizations such as holes and the functional groups which can increase or decrease the hydrophilicity of the adsorbent. The swelling index was measured by the following equation:
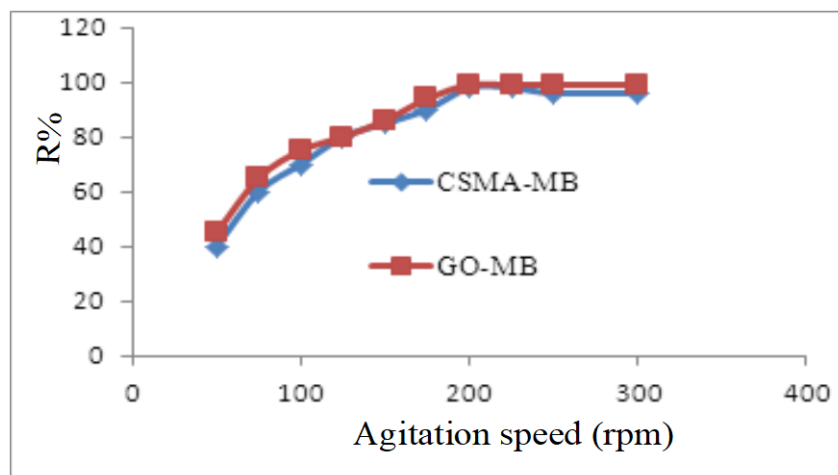
$$x = \frac{Mass\ of\ wet\ adsorbent - mass\ of\ dry\ adsorbent}{mass\ of\ dry\ adsorbent} \tag{1}$$
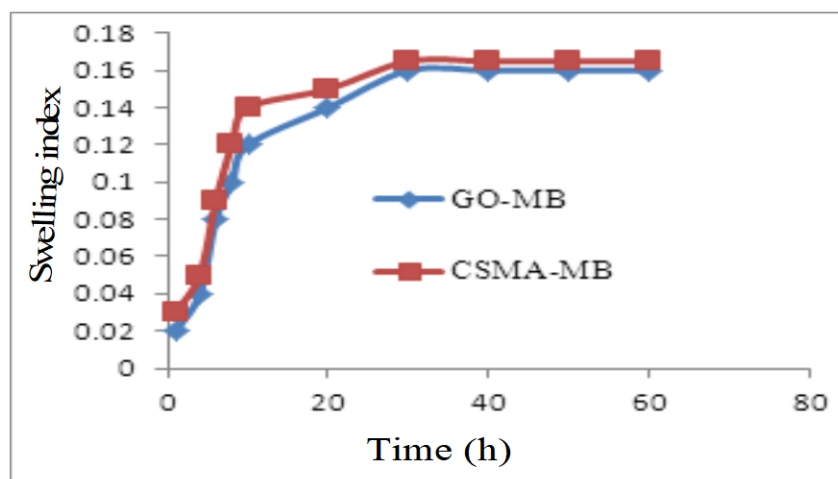
Modeling of adsorption isotherms

For the modeling of adsorption isotherm, we used the working solutions with zinc(II) ions contents of 40, 50, 80, 100, and 200 mg/L^{-1}. A standard $Zn(NO_3)_2.6H_2O$ was used for the preparation

Figure 6. Effect of concentration of Zn(II) ion on Zinc(II) ion adsorbent by CSMA-MB and GO-MB

Figure 7. Effect of agitation speed on Zinc(II) ion adsorbent by CSMA-MB and GO-MB

Figure 8. Swelling index of adsorbents (CSMA-MB and GO-MB)

of model zinc samples. The model metal samples with absorbent of concentration 10 g/L^{-1} were agitated in a shaking incubator at 200 rpm for CSMA-MB and 220 rpm for GO-MB till the uptake equilibrium was stabilized. At the times of establishing the uptake equilibrium which was set on the basis of kinetics study (1 h for CSMA- MB and 30 min for GO-MB), samples were drawn, filtered and analyzed using the method of atomic absorption spectrometry. Based on the acquired contents, zinc(II) ions adsorption was computed according to the following equation.

$$q_e = \frac{(C_o - C_e)\,V}{K} \tag{2}$$

where q_e is the equilibrium zinc(II) ion uptake (mg/g^{-1}), V the volume of zinc(II) ion solution (l); C_o and C_e are the initial and final zinc(II) ion concentration (mg/L^{-1}) and K is the weight of adsorbent (g). The best treatment to express zinc(II) ions adsorption from model solutions in all the adsorbent samples was the relation for modified langmuir isotherm of the first type equation 3:

$$q_e = \frac{q_{max} C_e K_L}{1 + K_L C_e} \tag{3}$$

Lined equation:

$$\frac{C_t}{q} = \frac{C_t}{q_m} + \frac{1}{K_L q_m} \tag{4}$$

where q is the equilibrium zinc(II) ion uptake (mg/g^{-1}), q_{max} is the maximum equilibrium metal uptake (mg/g^{-1}), K_L is the langmuir constant and C_t is the final zinc(II) ion concentration (mg/L^{-1}) (Figure 9).

The langmuir parameters can also be used to predict affinity between the adsorbent and the adsorbent using the dimension separation factor (R_L), which has been defined as below:

$$R_L = \frac{1}{1 + C_o K_L} \tag{5}$$

Where K_L is the langmuir constant (L/mg) C_o is the concentration of toxic heavy metal ions, in mg/L. The amount of R_L illustrated the type of the isotherm to be either undesirable ($R_L > 1$), linear ($R_L = 1$), desirable ($0 < R_L < 1$), or irreversible ($R_L = 0$). (Figure 10) illustrated that adsorption of zinc(II) ion was continually increased with a concentration of zinc(II) ion. The computed R_L value for zinc(II) ion adsorption illustrates that adsorption is desirable even for higher concentrations of zinc(II) ion [21, 22].

Adsorption zinc(II) ions isotherms were graphically created. The graphical representation of the linear form of langmuir adsorption isotherm model for the zinc(II) ions adsorption on the untreated and treated peat moss is illustrated in Figure 11, and the isotherm model parameters are summarized in Table 1 and Table 2. The change in the free energy (ΔG) was calculated from the langmuir constant using equation 6 and 7:

$$K_d = \frac{C_a}{C_s} \tag{6}$$

Where: C_a is the value of zinc(II) ions adsorbed at equilibrium C_s is the equilibrium concentration.

$$\Delta G = - RT \ln K_d \tag{7}$$

Where: R is the universal gas constant (8.314 J, $mole^{-1}$, K^{-1}) T is the absolute temperature. The negative values of ΔG (Table 2) are exhibited according to which the removal process of zinc(II) ions by adsorption on CSMA-MB and GO-MB are conceivable and immediate. In addition, the negative value of the ΔG obtained for the zinc(II) ions adsorption on CSMA-MB and GO-MB suggests that after the remedy, the accessibility of agent groups from the adsorbent surface will increase.
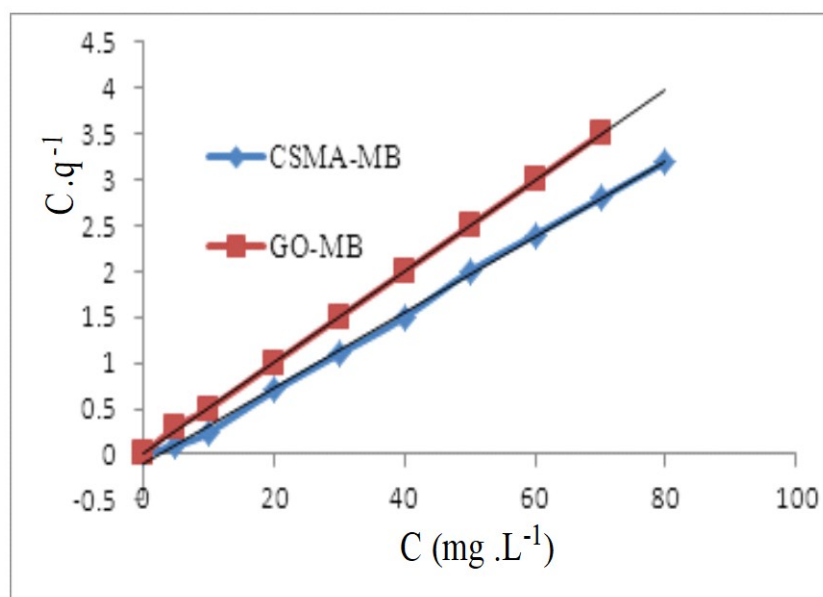
Desorption and repeated use

Desorption of zinc(II) ion was administered by 0.5M HNO_3 solution. The CSMA-M zinc(II) ion, complexes were immersed in 0.5M HNO_3 solutions and the mixture was shaken until equilibrium was reached (30 min). Then, the mixture was filtrated and the final concentrations of zinc(II) ion in the aqueous solution was measured by AAs. The desorption ratio (D%) of zinc(II) ion from the (CSMA-MB and GO-MB) adsorbents were computed by the following equation.
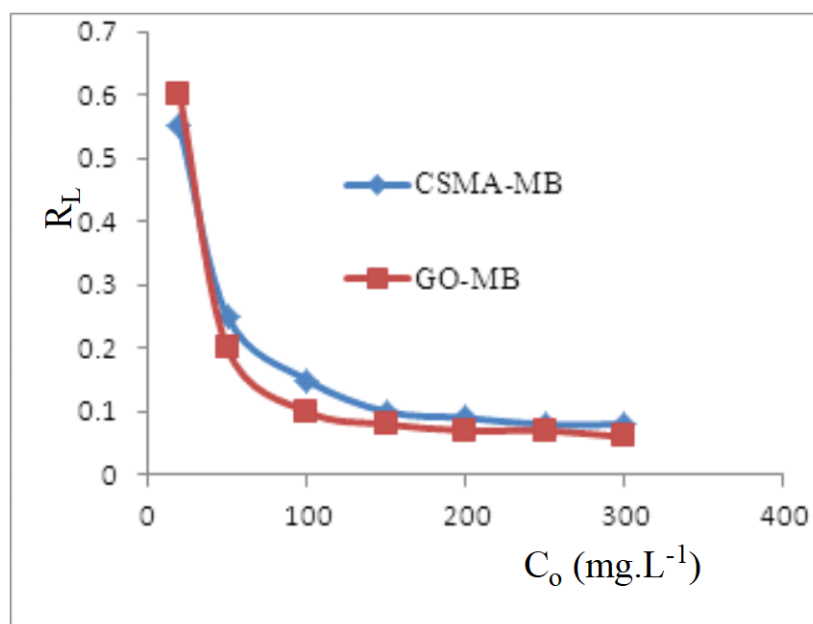
$$D\% = \frac{V_d C_d}{V(C_i - C_e)} \times 100 \tag{8}$$

Where: V is the volume of the solution (L); C_d is the concentration of the zinc(II) ions in the desorption solutions (mg/L); and V_d is the volume of the desorption solution (L). The assembled (CSMA-MB and GO-MB) from the desorption process was washed thoroughly with deionized water and dried by vacuum pump at 66 °C for repeated use [23–27].

Conclusion

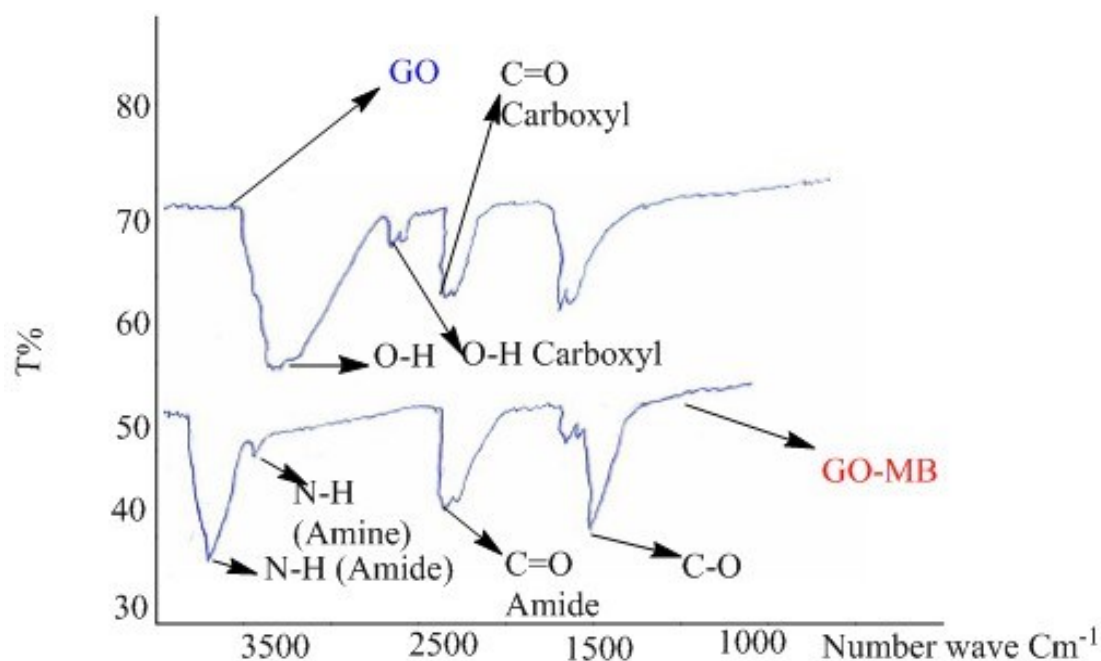**Figure 9.** Application of langmuir model for Zinc(II) ions adsorption on CSMA- MB and GO-MB

Figure 10. Separation factor (R_L) for adsorption of Zinc(II) ion as function of concentration of Zinc ion by CSMA-MB and GO-MB

Table 2. Isotherm constants for cobalt adsorption on studying adsorbents

Adsorbent	Regression Equation	R^2	q_{max}(mg.g^{-1})	K_L(L.mg^{-1})	R_L	ΔG(kj.mol^{-1})
CSMA-MB	Y=0.0213x +0.104	0.9982	46.95	2.05	0. 1	-11.38
GO-MB	Y= 0.0197x + 0.014	0.9998	50.76	1.41	0. 14	-13.11

Table 1. Optimized characters in this work

Adsorbent	pH	Swelling Index	Contact time (min)	Adsorbent dose (g.L⁻¹)	Initial concentration (mg.L⁻¹)	Agitation speed (rpm)
CSMA-MB	6	0.160	60	2.5	50	200
GO-MB	8	0.155	30	2.5	50	220

Figure 11. FT-IR spectrum of graphene oxide and GO-melamine butandioic acid

Application of adsorbents GO-MB and CSMA-MB for zinc(II) ion adsorption possesses a lot of advantages as compared to the classic methods such as chemical precipitation, membrane filtering, chemical oxidation or reduction, etc. Based on zinc(II) ion sorption capacity studies, it can be explained that GO-MB or CSMA-MB is a suitable sorbent for heavy metal ions such as zinc(II) ion. Adsorption of zinc(II) ion is found to be effective in the pH range 1-6 for CSMA-MB and 1-10 for GO-MB adsorbent. The adsorbents were resulted to be reproducible with a good zinc(II) ion selectivity over other potentially interfering ions. Data of these adsorbents readily set with langmuir isotherm. These adsorbents were tested on various water samples, which showed high adsorption capacity for the elimination of amounts zinc(II) ion. These adsorbents are very proper for removing zinc(II) ion from aqueous solutions.

The authors would like to appreciate Prof. M.A. Zanjanchi), Prof. M. Arvand, and Dr. Shabnam Sohrabnajad (Guilan University) for helping me on spectrophotometry.

Disclosure statement

No potential conflict of interest was reported by the authors.

References

[1]. Jeong E.Y., Ansari M.B., Mo Y.H., Park S.E. *J. Hazard. Mater.*, 2011, **185**:1311

[2]. Lee H.K., Song K., Seo H.R., Choi Y.K., Jeon S. *Sensor. Actuat. B,* 2004, **99**:323

[3]. Hummers W.S., Offeman R.E. *J. Am. Chem. Soc.*, 1958, **80**:1339

[4]. Stankovich S., Dikin D.A., Dommett G.H.B., Kohlhaas K.M., Zimney E.J., Stach E.A., Piner R.D., Nguyen S.T., Ruoff R.S. *Nature*, 2006, **442**:282

[5]. Liang X., Fu Z., Chou S.Y. *Nano Lett.*, 2007, **7**:3840

[6]. Berger C., Song Z., Li X., Wu X., Brown N., Naud C., Mayou D., Li T., Hass J., Marchenkov A.N., Conrad E.H., First P.N., Heer W.A. *Science*, 2006, **312**:1191

[7]. Sutter P.W., Flege J., Sutter E.A. *Nat. Mater.,* 2008, **7**:406

[8]. Demirbas A. *J. Hazard. Mater.*, 2008, **157**:9

[9]. Stankovich S., Piner R.D., Chen X., Wu N., Nguyen S.T., Ruoff R.S. *J. Mater. Chem.*, 2006, **16**:155

[10]. Stankovich S., Dikin D.A., Piner R.D., Kohlhaas K.A., Kleinhammes A., Jia Y., Wu Y., Nguyen S.T., Ruoff R.S. *Carbon*, 2007, **45**:1558

[11]. Cai D., Song M. *J. Mater. Chem.,* 2007, **17**:3678

[12]. Rostami H., Brooks R., Tovia F., Bahadory M. *J. Solid Waste Techn. Manag.*, 2009, **35**:127

[13]. Samadi N., Hasanzadeh R., Rasad M. *J. Appl. Polym. Sci.,* 2015*,* **132**, 41642.

[14]. Krishna M.B.M., Venkatramaiah N., Venkatesan R., Rao D.N. *J. Mater. Chem.*, 2012, **22**:3059

[15]. Hummers W.S., Offeman R.E. *J. Am. Chem. Soc.*, 1958, **80**:1339

[16]. Meena A.K., Kadirvelu K., Mishraa G.K., Rajagopal C., Nagar P.N. *J. Hazard. Mater.*, 2008, **150**:619

[17]. Sarý A., Uluozlü Ö.D., Tüzen M. *Chem. Eng. J.*, 2011, **167**:155

[18]. Iqbal, M. Saeed A., Edyvean R.G.J. *Chem. Eng . J.,* 2013, **225**: 192

[19]. Vinodhini V., Das N. *Int. J. Environ. Sci. Technol.*, 2010, **7**:85

[20]. Guo W., Chen R., Liu Y., Meng M., Meng X., Hu Z., Song Z. *Colloid. Surface. A, Physicochem. Eng. Asp.*, 2013, **436**:703

[21]. Abu Hasan H., Abdullah S.R., Kofli N.T., Kamarudin S.K. *J. Environ. Manage.,* 2012, **111**:34

[22]. El-Shafey E.I. *J. Hazard. Mater.*, 2010, **27**:319

[23]. Tunali Akar S., Arslan S., Alp T., Arslan D., Akar T. *Chem. Eng. J.,* 2012, **185**:92

[24]. Alomá I., Martín-Lara M.A., Rodríguez I.L., Blázquez G., Calero M. *J. Taiwan. Inst. Chem. Eng.*, 2012, **43**:275

[25]. Demirbas A. *J. Hazard. Mater.*, 2008, **157**:220

[26]. Wan Ngah W.S., Hanafiah M.A.K.M. *Bioresour. Technol.*, 2008, **99**:3935

[27]. Ahmaruzzaman M. *Adv. Colloid. Interface. Sci.*, 2011, **166**:59